

# Global status of neutrino oscillation parameters after Neutrino-2012

D. V. Forero,<sup>\*</sup> M. Tórtola,<sup>†</sup> and J. W. F. Valle<sup>‡</sup>

*AHEP Group, Instituto de Física Corpuscular – C.S.I.C./Universitat de València  
Edificio de Institutos de Paterna, Apartado 22085, E-46071 València, Spain*

Here we update the global fit of neutrino oscillations in Refs. [1, 2] including the recent measurements of reactor antineutrino disappearance reported by the Double Chooz, Daya Bay and RENO experiments, together with latest MINOS and T2K appearance and disappearance results, as presented at the Neutrino-2012 conference. We find that the preferred global fit value of  $\theta_{13}$  is quite large:  $\sin^2 \theta_{13} \simeq 0.025$  for normal and inverted neutrino mass ordering, with  $\theta_{13} = 0$  now excluded at more than  $10\sigma$ . The impact of the new  $\theta_{13}$  measurements over the other neutrino oscillation parameters is discussed as well as the role of the new long-baseline neutrino data and the atmospheric neutrino analysis in the determination of a non-maximal atmospheric angle  $\theta_{23}$ .

PACS numbers: 14.60.Pq, 13.15.+g, 26.65.+t, 12.15.Ff

Keywords: Neutrino mass and mixing; neutrino oscillation; solar and atmospheric neutrinos; reactor and accelerator neutrinos

## I. INTRODUCTION

Recent measurements of  $\theta_{13}$  have been reported by the reactor experiments Double Chooz [3], Daya Bay [4] and RENO [5]. These experiments look for the disappearance of reactor antineutrinos over baselines of the order of 1 km, due to neutrino oscillations mainly driven by the third mixing angle  $\theta_{13}$  of the lepton mixing matrix [6, 7]. Up to now the most sensitive measurements of reactor antineutrinos were reported by the past reactor experiments CHOOZ [8] and Palo Verde [9].

Compared to their predecessors, the new reactor experiments have larger statistics, thanks to their increased reactor power and the bigger antineutrino detector size. On the other hand, one of their most important features is that they have detectors located at different distances from the reactor core. As a result measurements at the closest detectors can be used in order to predict the expected event number at the more distant detectors, avoiding the need to rely on theoretical calculations of the produced antineutrino flux at the reactors. As a consequence these experiments have for the first time observed the disappearance of reactor antineutrinos over short distances, providing the first measurement of the mixing angle  $\theta_{13}$ , so far unknown.

Last year there were some indications for a non-zero  $\theta_{13}$  mixing angle coming from the observation of electron neutrino appearance on a muon neutrino beam at the accelerator oscillation experiments T2K [10] and MINOS [11]. Together with the hints from the solar and atmospheric neutrino data samples, the global analysis of neutrino oscillation data reported indications of non-zero  $\theta_{13}$  between  $3$  and  $4\sigma$ , depending on the treatment of short-baseline reactor data in the full analysis (see Refs [1, 2] for more details<sup>1</sup>). Here we update the global fit of neutrino oscillations given in Refs. [1, 2] by including the recent measurements of reactor antineutrino disappearance reported by the Double Chooz, Daya Bay and RENO experiments. In addition to the above-mentioned data our analysis includes also the most recent reactor neutrino data reported at the Neutrino-2012 Conference [14, 15], as well as the latest results of

---

<sup>\*</sup>Electronic address: [dvanegas@ific.uv.es](mailto:dvanegas@ific.uv.es)

<sup>†</sup>Electronic address: [mariam@ific.uv.es](mailto:mariam@ific.uv.es)

<sup>‡</sup>Electronic address: [valle@ific.uv.es](mailto:valle@ific.uv.es)

<sup>1</sup> Other recent global analyses previous to the Neutrino-2012 conference can be found in Refs.[12, 13]

the MINOS [16] and T2K [17, 18] experiments. The role of the new  $\theta_{13}$  measurements upon the determination of the remaining oscillation parameters is also analyzed. Particularly important is the impact of the new accelerator neutrino data as well as the details of the atmospheric neutrino analysis upon the determination of the atmospheric mixing angle  $\theta_{23}$ .

## II. REACTOR EXPERIMENTS: DOUBLE CHOOZ, DAYA BAY AND RENO

This year, in chronological order, the Double Chooz, Daya Bay and RENO Collaborations have reported measurements of the electron antineutrino disappearance with important levels of statistical significance.

The Double Chooz (DC) experiment, located in France, is a reactor experiment planned to have two detectors and two reactors. In its first stage DC has reported 101 days of running [3], with only the far detector operating so far. The near detector (ND) is expected to start operation by early 2013. The two reactors are approximately equal, with an individual power of  $4.25 \text{ GW}_{\text{th}}$  and are placed at a distance of 1050 m from the far detector. The detector has a fiducial volume of  $10 \text{ m}^3$  of neutrino target liquid. From the analysis of the rate and the energy spectrum of the prompt positrons produced by the reactor antineutrinos, the DC collaboration find  $\sin^2 2\theta_{13} = 0.086 \pm 0.041(\text{stat}) \pm 0.030(\text{syst})$ . Using only the ratio of observed to expected events they get a slightly higher best fit value:  $\sin^2 2\theta_{13} = 0.104 \pm 0.030(\text{stat}) \pm 0.076(\text{syst})$ . A more recent analysis of DC data with an exposure of 227.93 live days [14] has reported the observation of 8249 candidate electron antineutrinos while 8937 were expected in the absence of oscillations. Using a rate plus spectral shape analysis the following best fit value for the reactor angle is obtained:  $\sin^2 2\theta_{13} = 0.109 \pm 0.030(\text{stat}) \pm 0.025(\text{syst})$ .

The Daya Bay (DYB) reactor experiment [4] is a neutrino oscillation experiment designed to measure the mixing angle  $\theta_{13}$  as well. The experiment is placed in China and it contains an array of three groups of detectors and three groups of two-reactor cores. The far group of detectors (far hall) is composed of three detectors and the two near halls are composed by one and two detectors, respectively. In order to reduce systematic errors, the detectors are approximately equal, with a volume of 20 tons of Gadolinium-doped liquid scintillator as neutrino target material. The reactor cores are approximately equal as well, with a maximum power of  $2.9 \text{ GW}_{\text{th}}$  (total power of  $17.4 \text{ GW}_{\text{th}}$ ) and the distances to the detectors range from 350 to 2000 m approximately. The rate-only analysis performed by the DYB collaboration finds a best fit value of  $\sin^2 2\theta_{13} = 0.092 \pm 0.016(\text{stat}) \pm 0.005(\text{syst})$ . A zero value for  $\theta_{13}$  is excluded with a significance of  $5.2\sigma$ . New results presented in the Neutrino-2012 Conference [15] with 2.5 times more statistics allow a stronger rejection for  $\theta_{13} = 0$  that now is excluded at almost  $8\sigma$  by DYB alone. A rate-only statistical analysis of the new DYB data reports a best fit value of  $\sin^2 2\theta_{13} = 0.089 \pm 0.010(\text{stat}) \pm 0.005(\text{syst})$ .

The RENO experiment [5] is situated in South Korea and it has been running for 229 days. It shares some features with DC and DYB. RENO has six reactor cores, distributed along a 1.3 km straight line. Two of the reactors have a maximum power of  $2.66 \text{ GW}_{\text{th}}$  while the other four may reach  $2.8 \text{ GW}_{\text{th}}$ . Reactor antineutrinos are detected by two identical detectors, labeled as near and far, located at 294 and 1383 m from the reactor array center. Each RENO detector contains 16 tons of Gadolinium-doped Liquid Scintillator. Based on a rate-only analysis, the RENO Collaboration finds  $\sin^2 2\theta_{13} = 0.113 \pm 0.013(\text{stat.}) \pm 0.019(\text{syst.})$ , together with a  $4.9\sigma$  exclusion for  $\theta_{13} = 0$ .

### Reactor event calculation

Reactor antineutrinos are produced by the fission of the isotopes  $^{235}\text{U}$ ,  $^{239}\text{Pu}$ ,  $^{241}\text{Pu}$  and  $^{238}\text{U}$ . Each fissile isotope contributes to the total reactor neutrino flux and fuel content with a certain fission fraction  $f^l$  that can be calculated through a detailed simulation of the core evolution. After their production, the reactor antineutrinos are detected at the experiments via the inverse beta decay process, looking for a delayed coincidence between the positron annihilation and the neutron capture in the target material. The window of positron energy covered by the three experiments described above ranges from 0.7 to 12 MeV approximately.

For a given experiment, the total number of events expected at the  $i$ th detector coming from the  $r$ th reactor can be calculated as:

$$N_{i,r} = \frac{N_p P_{th}^r}{4\pi L_{ir}^2 \langle E_{fis} \rangle} \epsilon_i \int_0^\infty dE_\nu \Phi^r(E_\nu) \sigma_{IBD}(E_\nu) P(E_\nu, L_i) \quad (1)$$

where  $N_p$  is the number of protons in the target volume,  $P_{th}^r$  is the total reactor power,  $\epsilon_i$  denotes the efficiency of the detector and  $\langle E_{fis} \rangle = \sum_l f^l E_{fis}^l$  is the average energy released per fission, calculated from the individual fission fractions  $f^l$  and the energy release per fission for a given isotope  $l$  taken from Ref. [19]. For the antineutrino flux prediction  $\Phi^r(E_\nu)$  we use the recent parameterization given in Ref. [20] as well as the new normalization for reactor antineutrino fluxes updated in Ref. [21]. The inverse beta decay cross section  $\sigma_{IBD}(E_\nu)$  is taken from Ref. [22]. Finally, for the neutrino propagation factor  $P(E_\nu, L_{ir})$  we use the full three-neutrino disappearance probability. The distance between reactor and detector  $L_{ir}$  is also used to correct the total antineutrino flux at the detector site. In order to minimize the dependence upon the predicted normalization of the antineutrino spectrum, we analyze the total rate of expected events at the far detector/s in the presence of oscillations over the no-oscillation prediction. This way, our statistical analysis is free of correlations among the different reactor data samples, since the relative measurements do not rely on flux predictions.

### III. GLOBAL ANALYSIS

In our global analysis of neutrino oscillation parameters we combine the recent reactor data from Double Chooz, Daya Bay and RENO with all the remaining relevant experiments, as follows.

#### A. Solar neutrino and KamLAND data

We include the most recent solar neutrino data from the radiochemical experiments Homestake [23], Gallex/GNO [24] and SAGE [25], as well as the latest published data from Borexino [26], the three phases of the Super-Kamiokande experiment [27–29] and the three phases from the Sudbury Neutrino Experiment SNO [30, 31]. For our simulation of the production and propagation of neutrinos in the Sun we consider the most recent update of the standard solar model [32], fixing our calculations to the low metallicity model labeled as AGSS09. The impact of the choice of a particular solar model over the neutrino oscillation analysis has been discussed in the arXiv updated version of Ref. [33]. We also include the most recent results published by the KamLAND reactor experiment with a total livetime of 2135 days, including the data collected during the radiopurity upgrade in the detector [34].

#### B. Atmospheric and accelerator neutrino data

In our global fit we use the atmospheric neutrino analysis done by the Super-Kamiokande Collaboration [35]. The oscillation analysis has been performed within the one-mass scale approximation, neglecting the effect of the solar mass splitting and includes the atmospheric results from the three phases of the Super-Kamiokande experiment. Concerning the long-baseline data, we include the most recent results from the MINOS and T2K long-baseline experiments released last June at the Neutrino 2012 Conference. We consider the appearance and disappearance channels for both experiments as well as the neutrino and antineutrino data for MINOS. These new long-baseline results imply some improvements with respect to the previous MINOS and T2K data in Refs. [10, 11, 36–38]. On the one hand, the new results on  $\nu_\mu \rightarrow \nu_e$  appearance searches allow a better determination of the  $\theta_{13}$  mixing angle, although its current determination is fully dominated by the Daya Bay reactor data. On the other hand, and here lies the most relevant implication of the new long-baseline data, they show a preference for a non-maximal atmospheric mixing angle  $\theta_{23}$  in the  $\nu_\mu$  and  $\bar{\nu}_\mu$  channels. The impact of this preference on the determination of  $\theta_{23}$  in our global fit will be discussed in the next section.

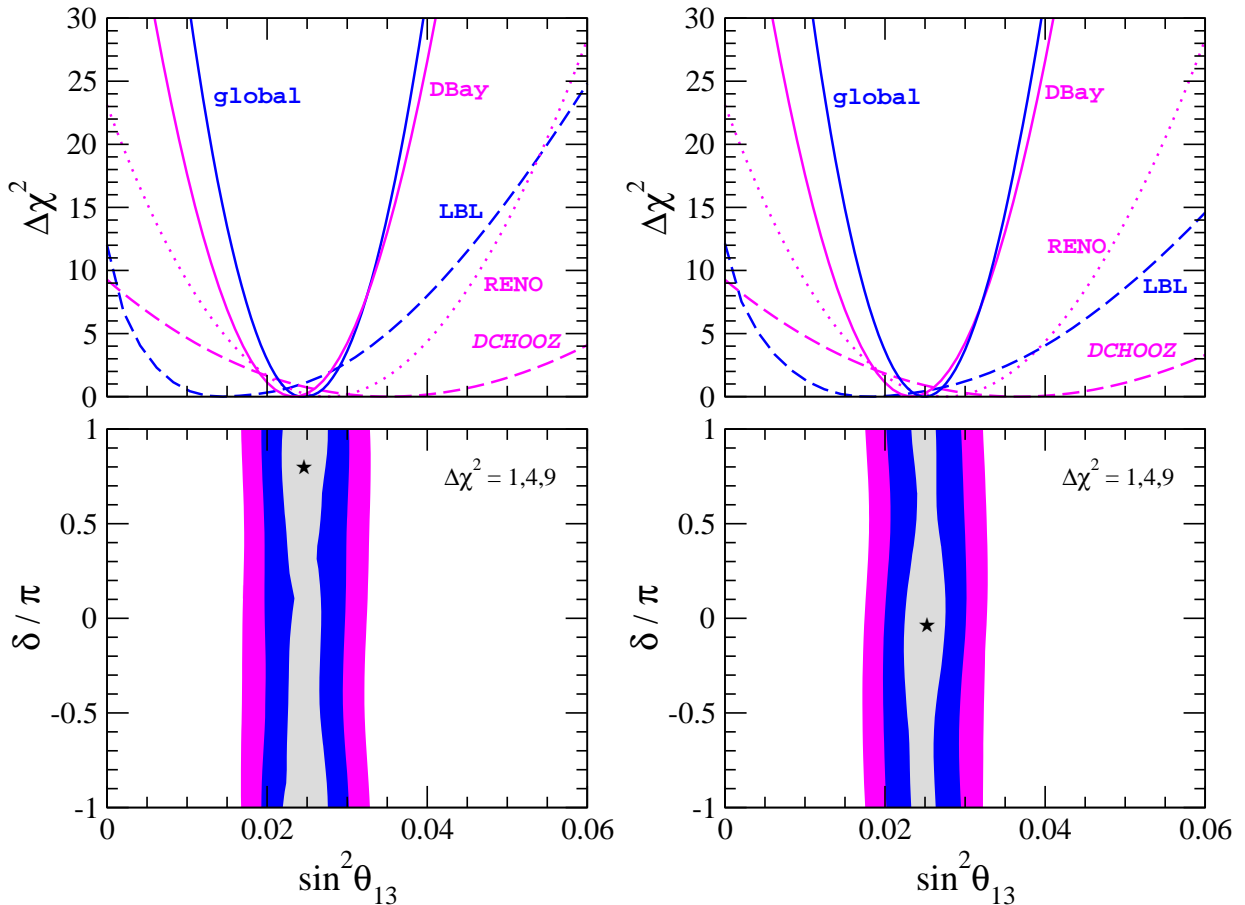


FIG. 1: Upper panels:  $\Delta\chi^2$  as a function of  $\sin^2\theta_{13}$  from the analysis of the total event rate in Daya Bay (solid magenta/light line), RENO (dotted line) and Double Chooz (dashed magenta/light line) as well as from the analysis of long-baseline (dashed blue/dark line) and global neutrino data (solid blue/dark line). Except for the case of the global fit here we have fixed the remaining oscillation parameters to their best fit values. Lower panels: contours of  $\Delta\chi^2 = 1, 4, 9$  in the  $\sin^2\theta_{13} - \delta$  plane from the global fit to the data. We minimize over all undisplayed oscillation parameters. Left (right) panels are for normal (inverted) neutrino mass hierarchy.

### C. Global fit results

Here we summarize the results for the neutrino oscillation parameters obtained in our present global analysis. For details on the numerical analysis of all the neutrino samples see Refs. [1, 2, 33, 39] and references therein.

The results obtained for  $\sin^2\theta_{13}$  and  $\delta$  are summarized in Fig. 1. In the upper panels we show the  $\Delta\chi^2$  profile as a function of  $\sin^2\theta_{13}$  for normal (left panel) and inverted (right panel) neutrino mass hierarchies. The solid blue/dark line corresponds to the result obtained from the combination of all the data samples while the others correspond to the individual reactor data samples and the combination of the long-baseline MINOS and T2K appearance and disappearance data, as indicated. One sees from the constraints on  $\sin^2\theta_{13}$  coming from the different data samples separately that, as expected, the global constraint on  $\theta_{13}$  is dominated by the recent Daya Bay measurements. For both neutrino mass hierarchies we find that the  $3\sigma$  indication for  $\theta_{13} > 0$  obtained in our previous work [2] due mainly to the first indications observed by MINOS and T2K is now overwhelmingly confirmed as a result of the recent reactor data. Thus, in our global fit we obtain a  $\Delta\chi^2 \sim 104$ , resulting in a  $10.2\sigma$  exclusion of  $\theta_{13} = 0$  for both mass hierarchies. In the lower panels of Fig. 1 we show the contours of  $\Delta\chi^2 = 1, 4, 9$  in the  $\sin^2\theta_{13} - \delta$  plane from the

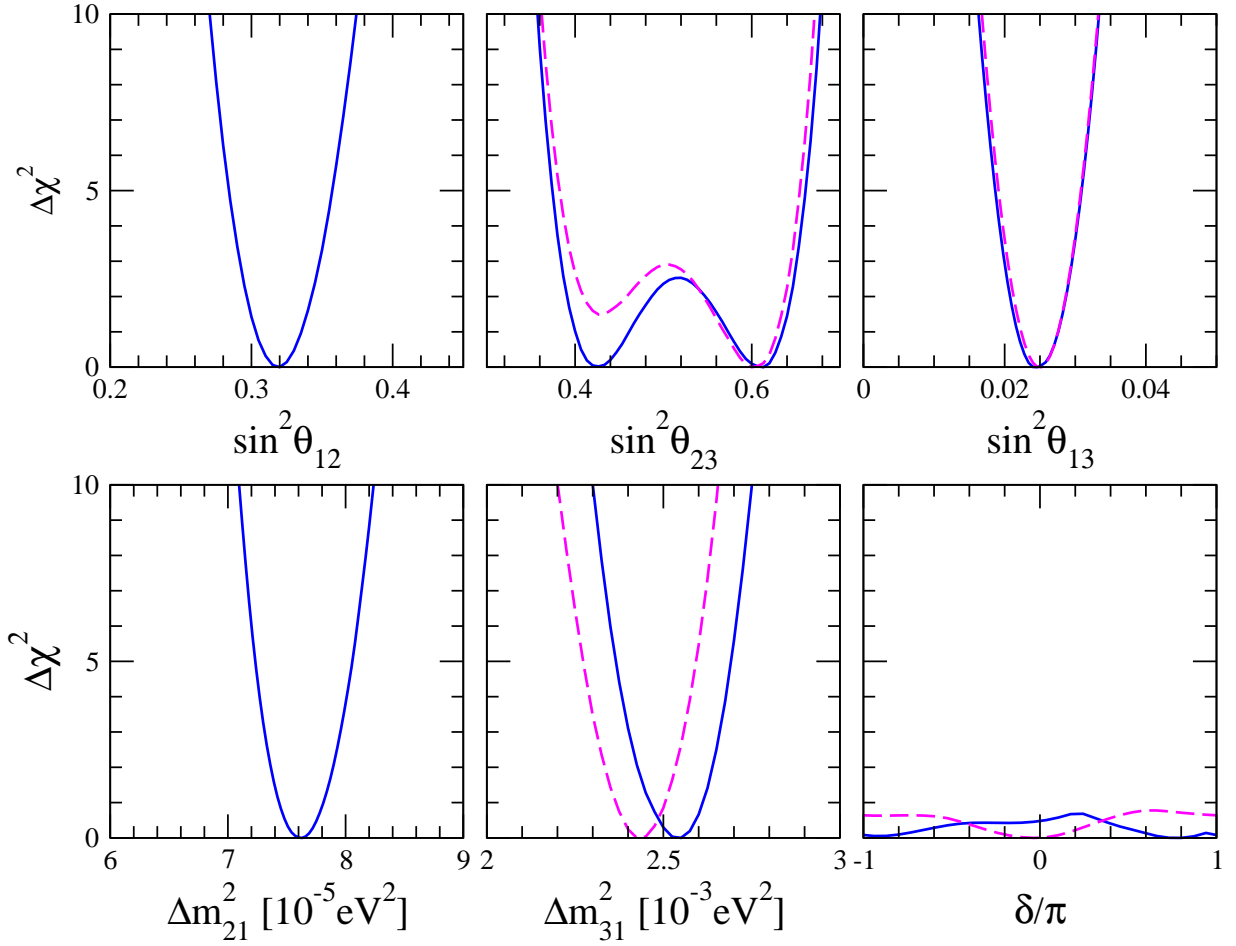


FIG. 2:  $\Delta\chi^2$  profiles as a function of all the neutrino oscillation parameters  $\sin^2 \theta_{12}$ ,  $\sin^2 \theta_{23}$ ,  $\sin^2 \theta_{13}$ ,  $\Delta m_{21}^2$ ,  $\Delta m_{31}^2$  and  $\delta$ . For the central and right panels the solid lines correspond to the case of normal mass hierarchy while the dashed lines correspond to the results for the inverted mass hierarchy.

global fit to the neutrino oscillation data. In this plane we find the following best fit points:

$$\sin^2 \theta_{13} = 0.0246, \quad \delta = 0.80\pi \quad (\text{normal hierarchy}), \quad (2)$$

$$\sin^2 \theta_{13} = 0.0250, \quad \delta = -0.03\pi \quad (\text{inverted hierarchy}). \quad (3)$$

In our previous analysis [2] there was a “preferred region” at  $\Delta\chi^2 = 1$  for the CP phase  $\delta$  for normal neutrino mass ordering, as a result of the complementarity between MINOS and T2K appearance data. One sees that this effect has been diluted after the combination with the new reactor data, so no “preferred region” for the CP phase  $\delta$  remains at  $\Delta\chi^2 = 1$ <sup>2</sup>. For this reason we marginalize over the CP phase  $\delta$  (and all other oscillation parameters), obtaining for the best fit, one-sigma errors, and the significance for  $\theta_{13} > 0$ :

$$\begin{aligned} \sin^2 \theta_{13} &= 0.0246^{+0.0029}_{-0.0028}, & \Delta\chi^2 &= 103.5 (10.2\sigma) & (\text{normal}), \\ \sin^2 \theta_{13} &= 0.0250^{+0.0026}_{-0.0027}, & \Delta\chi^2 &= 104.7 (10.2\sigma) & (\text{inverted}). \end{aligned} \quad (4)$$

When compared with the previous analysis in Refs. [1, 2], we remark that here we are not including previous short baseline reactor experiments, which would lead to a somewhat less significant result for the exclusion of  $\theta_{13} = 0$ .

<sup>2</sup> Note that, given the approximations adopted in the atmospheric neutrino analysis in Ref. [35], the sensitivity to the parameter  $\delta$  in our global fit comes only from long-baseline neutrino data.

parameter	best fit	1 $\sigma$ range	2 $\sigma$ range	3 $\sigma$ range
$\Delta m_{21}^2$ [ $10^{-5}\text{eV}^2$ ]	7.62	7.43–7.81	7.27–8.01	7.12–8.20
$ \Delta m_{31}^2 $ [ $10^{-3}\text{eV}^2$ ]	2.55	2.46 – 2.61	2.38 – 2.68	2.31 – 2.74
	2.43	2.37 – 2.50	2.29 – 2.58	2.21 – 2.64
$\sin^2 \theta_{12}$	0.320	0.303–0.336	0.29–0.35	0.27–0.37
$\sin^2 \theta_{23}$	0.613 (0.427) <sup>a</sup>	0.400–0.461 & 0.573–0.635	0.38–0.66	0.36–0.68
	0.600	0.569–0.626	0.39–0.65	0.37–0.67
$\sin^2 \theta_{13}$	0.0246	0.0218–0.0275	0.019–0.030	0.017–0.033
	0.0250	0.0223–0.0276	0.020–0.030	
$\delta$	$0.80\pi$	$0 - 2\pi$	$0 - 2\pi$	$0 - 2\pi$
	$-0.03\pi$			

<sup>a</sup>This is a local minimum in the first octant of  $\theta_{23}$  with  $\Delta\chi^2 = 0.02$  with respect to the global minimum

TABLE I: Neutrino oscillation parameters summary. For  $\Delta m_{31}^2$ ,  $\sin^2 \theta_{23}$ ,  $\sin^2 \theta_{13}$ , and  $\delta$  the upper (lower) row corresponds to normal (inverted) neutrino mass hierarchy.

Besides  $\theta_{13}$  and  $\delta$ , from the global analysis of neutrino data we also recalculate the best fit values and ranges allowed for all the other neutrino oscillation parameters. Our results are summarized in Fig. 2 and Table I.

Comparing with our previous results we see that the inclusion of the new reactor and long-baseline data does not have a strong impact on the determination of the solar neutrino oscillation parameters, which are already pretty well determined by solar and KamLAND reactor data. The differences between the results in Table I and those in Table I in [2] are due to the different treatment of reactor data. Indeed, motivated by the so-called “reactor antineutrino anomaly” [40], old data from reactor experiments were included in the analysis in [2]. The dependence of the determination of solar neutrino oscillation parameters  $\sin^2 \theta_{12}$  and  $\Delta m_{21}^2$  upon the details of the reactor data analysis has already been discussed in detail in Ref. [1].

Concerning atmospheric neutrino parameters, the best fit values for the atmospheric mass splitting parameter  $\Delta m_{31}^2$  in Tab. I have been shifted to somewhat larger values compared to our previous results in Ref. [2]. This is mainly due to the new MINOS disappearance data in Ref. [16], that prefer values for the mass splitting parameter larger than in their previous data release in [36]. The precision in the determination of  $\Delta m_{31}^2$  has also been improved thanks to the new long-baseline neutrino data. Thus, at  $3\sigma$  we find approximately a 8% accuracy in the determination of  $\Delta m_{31}^2$ , while a 12% accuracy was obtained in [2] at  $3\sigma$ . For the atmospheric mixing angle we note a slight rejection for maximal values of  $\theta_{23}$ . In particular, our global fit shows a preference for the mixing angle in the second octant. This preference is very weak for the normal mass hierarchy case, where a local best fit point at  $\sin^2 \theta_{23} = 0.427$  appears with  $\Delta\chi^2 \simeq 0.02$ , so that a symmetric  $\Delta\chi^2$  profile can be seen at middle-top panel of Fig. 2. For inverted mass ordering however, the profile is more asymmetric and a local minimum for  $\theta_{23}$  appears in the first octant only at  $\Delta\chi^2 \simeq 1.5$ . Maximal mixing, i.e.  $\theta_{23} = \pi/4$  is disfavoured at  $\sim 90\%$  C.L. for both hierarchies. While the preference for non-maximal values of the atmospheric mixing angle comes directly from the new MINOS data, the choice of a particular octant comes from the interplay of long-baseline, reactor and atmospheric neutrino data, as we will discuss in detail in the next section.

#### IV. DISCUSSION

We now discuss the impact of the new long-baseline data and the atmospheric neutrino analysis in the determination of the atmospheric mixing parameter  $\theta_{23}$ . As already stated above the new disappearance data from MINOS show a preference for non-maximal values of  $\theta_{23}$ . Due to the smallness of the associated matter effects in MINOS, these data

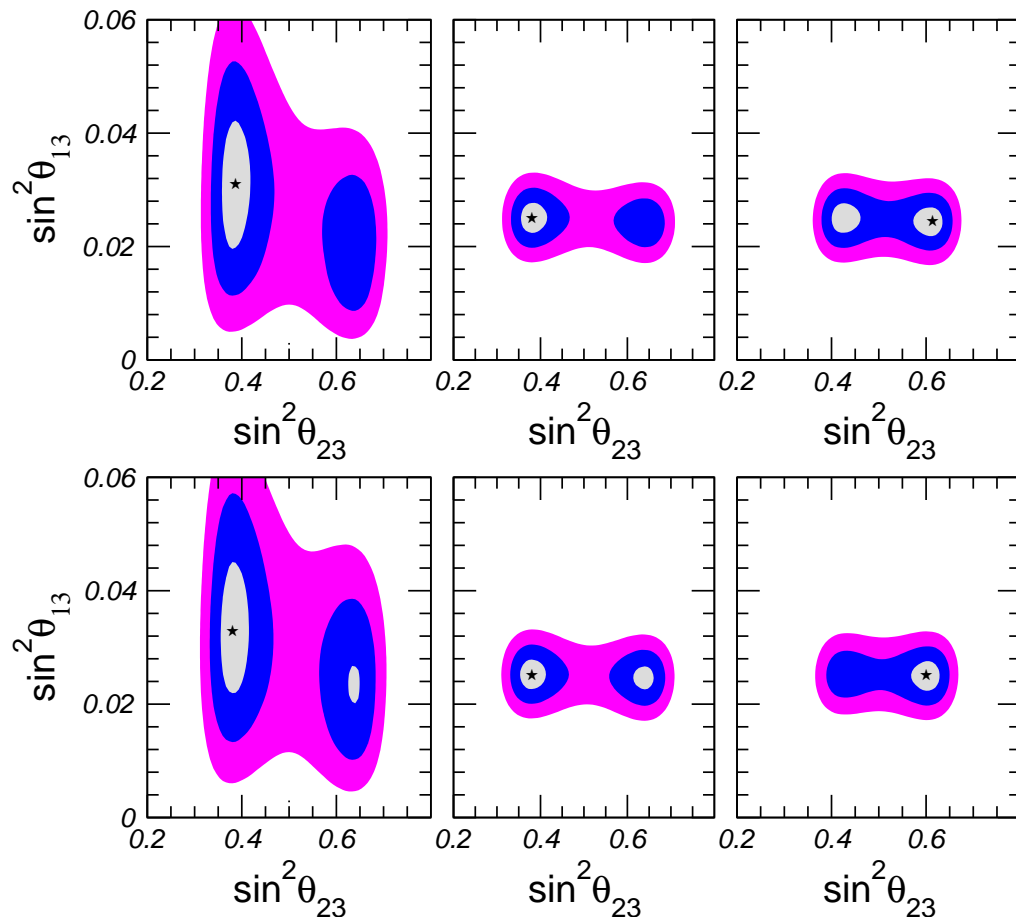


FIG. 3: Upper panels: contour regions with  $\Delta\chi^2 = 1, 4, 9$  in the  $\sin^2\theta_{23} - \sin^2\theta_{13}$  plane from the analysis of long-baseline (MINOS and T2K) + solar + KamLAND data (left panel), long-baseline + solar + KamLAND + new Double Chooz, Daya Bay and RENO reactor data (middle panel) and the global combination (right panel) for normal hierarchy. Lower panels, same but for (inverted) neutrino mass hierarchy.

are octant-symmetric and therefore say nothing about the octant of the atmospheric mixing angle  $\theta_{23}$ . However, the interplay with long-baseline neutrino appearance and reactor antineutrino data breaks the octant-degeneracy, leading to a small preference for values of  $\theta_{23}$  smaller than  $\pi/4$ . This is seen in the left panels of Fig. 3 where we have plotted the allowed regions in the  $\sin^2\theta_{23} - \sin^2\theta_{13}$  plane from the combination of long-baseline (MINOS and T2K) with solar + KamLAND. These data samples prefer  $\theta_{23}$  values in the first octant and the same holds for the case when new reactor data are included, see middle panels in Fig. 3. Up to this point all statistical analysis are in agreement [41, 42].

Nevertheless, when we then include atmospheric data in the global analysis, differences in the determination of  $\theta_{23}$  arise due to the differences in the analysis of atmospheric neutrino data. In fact, one sees that the effect of combining with the atmospheric neutrino data maintains the preference for non-maximal values of  $\theta_{23}$  but leads to a shift towards  $\sin^2\theta_{23}$  in the second octant for both mass orderings, as seen in the right panels in Fig. 3. In contrast Refs. [41, 42] find  $\theta_{23}$  in the first octant for both spectra. Note however that the preference for a given octant in our analysis is still rather marginal, and  $\theta_{23}$  values in the first octant appear with  $\Delta\chi^2 = 0.02$  and 1.5 for normal and inverse mass hierarchy respectively.

As stated in Section III B, for our global fit we use the official Super-Kamiokande analysis of atmospheric neutrino data in Ref. [35], performed within the one-mass scale approximation. This analysis shows a preference for maximal  $\theta_{23}$  mixing, although a small deviation of  $\theta_{23}$  to the second octant is found in the case of inverse mass ordering. The most recent analysis of the Super-Kamiokande collaboration presented in Neutrino-2012 [43] and performed with



the inclusion of solar mass splitting corrections is in agreement with their previous results (obtained without these corrections). In this case a small preference for  $\theta_{23}$  in the first octant for the normal spectrum, and for second octant for the inverted one is found, with maximal mixing well inside the one sigma range. In contrast, the analyses of Refs. [41, 42], updated after Neutrino-2012, find a global preference for  $\theta_{23}$  in the first octant and exclude maximal mixing at the  $2\sigma$  level (for normal hierarchy), in qualitative agreement with each other, though the agreement is not perfect at the quantitative level. Both of these analyses are at odds with the latest Super-Kamiokande atmospheric neutrino data analysis in [43]. At the moment it is not clear what is the origin of this discrepancy.

The impact of the atmospheric neutrino analysis upon the determination of  $\theta_{23}$  is very visible, therefore in order to get a robust measurement of the atmospheric mixing angle it is crucial to clarify the origin of the discrepancies among the various analysis of atmospheric data.

## V. CONCLUSION AND OUTLOOK

We have updated the global fit of neutrino oscillation parameters including the recent measurements of reactor antineutrino disappearance reported by the Double Chooz, Daya Bay and RENO experiments, as well as latest MINOS and T2K appearance and disappearance results, as presented at the Neutrino-2012 conference. We have found that the preferred global fit value of  $\theta_{13}$  is  $\sin^2 \theta_{13} = 0.0246(0.0250)$  for normal (inverted) neutrino mass hierarchy, while  $\sin^2 \theta_{13} = 0$  is now excluded at  $10.2\sigma$ . There is reasonable agreement with the results of other global analyses [41, 42], except for the atmospheric neutrino mixing parameter. We find that the global analysis pushes the atmospheric mixing angle  $\sin^2 \theta_{23}$  best fit value towards the second octant for both neutrino mass orderings. This hint, however, is still quite marginal and first-octant values of  $\theta_{23}$  are well inside the  $1\sigma$  range for normal hierarchy and at  $1.2\sigma$  for the inverted spectrum. Independent phenomenological analyses of atmospheric neutrino data in Refs. [41, 42] obtain a preference for mixing angle in the first octant for both mass hierarchies. Moreover, the new official Super-Kamiokande analysis in Ref. [43] with full three flavour effects gives a somewhat weaker preference for non-maximal  $\theta_{23}$  mixing, together with a correlation between the neutrino mass ordering and the preferred octant for  $\theta_{23}$ . The origin of this discrepancy which crucially affects the determination of the atmospheric mixing angle is not yet clear. The impact of the new reactor and long-baseline accelerator measurements upon the solar neutrino oscillation parameters is completely marginal, the results are summarized in Table I.

During the summer this year the Daya Bay Collaboration will complete the designed number of detectors by adding one detector in the far hall and other one in one of the near halls, re-starting the data taking after summer with eight neutrino detectors. After 3 years of operation the uncertainties on  $\sin^2 2\theta_{13}$  will be reduced from 20% to 4-5% [44]. Needless to say that a good determination of a sizeable  $\theta_{13}$  value will be a crucial ingredient towards a new era of CP violation searches in neutrino oscillations [45, 46] and will also help determining the neutrino mass hierarchy.

Note added: During the refereeing process of the present work, a new analysis has appeared in Ref. [47]. The authors obtain a preference for non-maximal values of  $\theta_{23}$  at the  $1.7-2\sigma$  level as a result of the new MINOS disappearance data. Their new atmospheric neutrino data analysis results in a reduced sensitivity to the  $\theta_{23}$  octant in their global fit, in better agreement with the analysis by the Super-K collaboration than their previous results given in [42].

## Acknowledgments

This work was supported by the Spanish MINECO under grants FPA2011-22975 and MULTIDARK CSD2009-00064 (Consolider-Ingenio 2010 Programme), by Prometeo/2009/091 (Generalitat Valenciana) and by the EU ITN UNILHC PITN-GA-2009-237920. M.T. acknowledges financial support from CSIC under the JAE-Doc programme,



co-funded by the European Social Fund.

- 
- [1] T. Schwetz, M. Tortola and J. W. F. Valle, *New J. Phys.* **13**, 063004 (2011), [1103.0734].
- [2] T. Schwetz, M. Tortola and J. W. F. Valle, *New J.Phys.* **13**, 109401 (2011), [1108.1376].
- [3] DOUBLE-CHOOZ Collaboration, Y. Abe *et al.*, *Phys.Rev.Lett.* **108**, 131801 (2012), [1112.6353].
- [4] DAYA-BAY Collaboration, F. An *et al.*, *Phys.Rev.Lett.* **108**, 171803 (2012), [1203.1669].
- [5] RENO collaboration, J. Ahn *et al.*, 1204.0626.
- [6] J. Schechter and J. W. F. Valle, *Phys. Rev.* **D22**, 2227 (1980); W. Rodejohann & J. Valle, *Phys.Rev.* **D84**, 073011 (2011).
- [7] K. Nakamura *et al.*, *Journal of Physics G: Nuclear and Particle Physics* **37**, 075021 (2010).
- [8] CHOOZ Collaboration, M. Apollonio *et al.*, *Eur. Phys. J.* **C27**, 331 (2003), [hep-ex/0301017].
- [9] Palo Verde Collaboration, F. Boehm *et al.*, *Phys. Rev.* **D64**, 112001 (2001), [hep-ex/0107009].
- [10] T2K Collaboration, K. Abe *et al.*, *Phys.Rev.Lett.* **107**, 041801 (2011), [1106.2822].
- [11] MINOS Collaboration, P. Adamson *et al.*, *Phys.Rev.Lett.* **107**, 181802 (2011), [1108.0015].
- [12] M. Gonzalez-Garcia, M. Maltoni and J. Salvado, *JHEP* **1004**, 056 (2010), [1001.4524].
- [13] G. Fogli, E. Lisi, A. Marrone, A. Palazzo and A. Rotunno, *Phys.Rev.* **D84**, 053007 (2011), [1106.6028].
- [14] M. Ishitsuka's talk at Neutrino 2012 conference, Kyoto, June 2012 Y. Abe *et al.*, arXiv:1207.6632 [hep-ex].
- [15] D. Dwyer's talk at Neutrino 2012 conference, Kyoto, June 2012
- [16] R. Nichol's talk at Neutrino 2012 conference, Kyoto, June 2012
- [17] K. Abe *et al.* [T2K Collaboration], *Phys. Rev. D* **85**, 031103 (2012) [arXiv:1201.1386 [hep-ex]].
- [18] T. Nakaya's talk at Neutrino 2012 conference, Kyoto, June 2012.
- [19] V. Kopeikin, L. Mikaelyan and V. Sinev, *Phys.Atom.Nucl.* **67**, 1892 (2004), [hep-ph/0410100].
- [20] T. Mueller *et al.*, *Phys.Rev.* **C83**, 054615 (2011), [1101.2663].
- [21] K. N. Abazajian *et al.*, arXiv:1204.5379 [hep-ph].
- [22] P. Vogel and J. F. Beacom, *Phys. Rev.* **D60**, 053003 (1999), [hep-ph/9903554].
- [23] B. T. Cleveland *et al.*, *Astrophys. J.* **496**, 505 (1998).
- [24] F. Kaether, W. Hampel, G. Heusser, J. Kiko and T. Kirsten, *Phys.Lett.* **B685**, 47 (2010), [1001.2731].
- [25] SAGE Collaboration, J. N. Abdurashitov *et al.*, *Phys. Rev.* **C80**, 015807 (2009), [0901.2200].
- [26] G. Bellini *et al.* [The Borexino Collaboration], *Phys. Rev. Lett.* **107** (2011) 141302 [arXiv:1104.1816 [hep-ex]].
- [27] Super-Kamiokande Collaboration, J. Hosaka *et al.*, *Phys. Rev.* **D73**, 112001 (2006), [hep-ex/0508053].
- [28] J. P. Cravens *et al.* [Super-Kamiokande Collaboration], *Phys. Rev. D* **78** (2008) 032002 [arXiv:0803.4312 [hep-ex]].
- [29] Super-Kamiokande Collaboration, K. Abe *et al.*, *Phys.Rev.* **D83**, 052010 (2011), [1010.0118].
- [30] SNO Collaboration, B. Aharmim *et al.*, *Phys. Rev. Lett.* **101**, 111301 (2008), [0806.0989].
- [31] SNO Collaboration, B. Aharmim *et al.*, *Phys. Rev.* **C81**, 055504 (2010), [0910.2984].
- [32] A. Serenelli, S. Basu, J. W. Ferguson and M. Asplund, *Astrophys.J.* **705**, L123 (2009), [0909.2668].
- [33] T. Schwetz, M. Tortola and J. W. F. Valle, *New J. Phys.* **10**, 113011 (2008), [0808.2016].
- [34] The KamLAND Collaboration, A. Gando *et al.*, *Phys.Rev.* **D83**, 052002 (2011), [1009.4771].
- [35] Super-Kamiokande Collaboration, R. Wendell *et al.*, *Phys.Rev.* **D81**, 092004 (2010), [1002.3471].
- [36] MINOS Collaboration, P. Adamson *et al.*, *Phys.Rev.Lett.* **106**, 181801 (2011), [1103.0340].
- [37] MINOS collaboration, P. Adamson *et al.*, *Phys.Rev.Lett.* **107**, 021801 (2011), [1104.0344].
- [38] MINOS Collaboration, P. Adamson *et al.*, *Phys. Rev. Lett.* **108**, 191801 (2012), [1202.2772].
- [39] M. Maltoni, T. Schwetz, M. A. Tortola and J. W. F. Valle, *New J. Phys.* **6**, 122 (2004), hep-ph/0405172.
- [40] G. Mention *et al.*, *Phys. Rev.* **D83**, 073006 (2011), [1101.2755].
- [41] G. L. Fogli, E. Lisi, A. Marrone, D. Montanino, A. Palazzo and A. M. Rotunno, *Phys. Rev. D* **86** (2012) 013012 [arXiv:1205.5254 [hep-ph]].
- [42] T. Schwetz's talk at "What's  $\nu$ " workshop, Florence, June 2012.
- [43] Y. Itow's talk at Neutrino 2012 conference, Kyoto, June 2012.
- [44] J. Cao's talk at nuTURN2012 - Neutrino at the Turning Point, Gran Sasso, May 2012.
- [45] H. Nunokawa, S. J. Parke and J. W. F. Valle, *Prog. Part. Nucl. Phys.* **60**, 338 (2008).
- [46] ISS Physics Working Group, A. Bandyopadhyay *et al.*, *Rept.Prog.Phys.* **72**, 106201 (2009), [0710.4947].
- [47] M. C. Gonzalez-Garcia, M. Maltoni, J. Salvado and T. Schwetz, arXiv:1209.3023 [hep-ph].